Hindawi
International Journal of Antennas and Propagation
Volume 2022, Article ID 8294000, 7 pages
https://doi.org/10.1155/2022/8294000

Research Article

On the Voltage Response of Homogeneous Earth Models in Central Loop Electromagnetic Sounding

Mauro Parise

Faculty of Engineering, University Campus Bio-Medico of Rome Via Alvaro Del Portillo 21, Rome 00128, Italy

Correspondence should be addressed to Mauro Parise; m.parise@unicampus.it

Received 10 February 2022; Accepted 6 May 2022; Published 16 June 2022

Academic Editor: Anna Pietrenko-Dabrowska

An accurate series-form explicit expression is derived for the voltage induced in the small receiving loop of a central loop electromagnetic sounding system positioned above a homogeneous earth model. The solution is obtained by converting the semi-infinite integral representation for the vertical magnetic field induced at the center of the two loops into a series of simpler integrals, amenable to analytical evaluation. The developed formulation is based on replacing the exponential term in the integrand of the field integral with its power series expansion with respect to the difference of the squares of the wavenumbers in air and in the conducting medium. As a result, the vertical magnetic field and the induced voltage are finally expressed as sums of the spherical Hankel functions depending on geometrical parameters and the wavenumbers. The derived solution exhibits advantages in terms of both time cost and accuracy, when compared to the conventional numerical schemes for evaluating the Sommerfeld-type integrals and to the previously published quasistatic solution to the considered problem.

1. Introduction

Central loop electromagnetic sounding is a widespread technique for the exploration of earth structures, which consists of interpreting a set of measurements of the voltage induced in a small receiving loop placed at the center of a larger transmitting loop [1–17]. The underlying concept is that the presence of buried objects or other inhomogeneities in the subsurface structures may be revealed by the discrepancy between the recorded experimental data and the theoretical response curves associated with different earth models [8, 11–13, 18]. This implies that correct data interpretation requires the a priori knowledge of highly accurate theoretical response curves, at least for the standard homogeneous earth model. Yet, despite this necessity, only under the quasistatic field assumption can we derive an accurate analytical solution for the time-harmonic voltage induced in the receiver of a transmitter-receiver loop system located on a homogeneous ground. Thus, when the quasistatic assumption fails, the induced voltage is typically through time-consuming numerical approaches or 3D electromagnetic software tools [5, 13]. An attempt to overcome the restrictions implied by the quasistatic assumption and, at the same time, providing an efficient method to compute the voltage induced in the receiver has been made in [2], where a hybrid analytical-numerical solution valid for the general case of multilayer ground has been proposed. The solution has been shown to be robust and efficient but it suffers from the limitation that its usage requires the a priori computation of a set of numerical coefficients through an expensive iterative optimization algorithm.

The purpose of this work is to derive the exact series-form explicit solution describing the voltage response of a central-loop electromagnetic sounding system positioned on a homogeneous medium. The solution is obtained by converting the semi-infinite integral representation for the vertical magnetic field induced at the center of the two loops into a series of simpler integrals, amenable to analytical evaluation. The developed formulation is based on replacing the exponential term in the integrand of the field integral with its power series expansion with respect to the difference of the squares of the wavenumbers in air and in the conducting medium. As a result, the field and the voltage are

expressed in terms of spherical Hankel functions of the wavenumbers and geometrical parameters. The obtained solution is not subject to the quasistatic assumption and is valid in a wide frequency range. Numerical tests are carried out to illustrate the advantages of the proposed approach. In particular, the comparison with the outcomes from the previously published quasistatic solution reveals the failure of the latter even in the low-frequency range. This evidence further confirms the usefulness of the derived expressions for the vertical magnetic field produced at the center of the two loops and the voltage induced in the small receiving loop.

2. Theory

Consider a current-carrying circular loop antenna and a co-axial and co-planar small receiving loop located at height $d \longrightarrow 0$ above a homogeneous earth structure as sketched in Figure 1. The dielectric permittivity and electric conductivity of the ground are denoted by ϵ_1 and σ_1 , respectively, while the magnetic permeability is assumed to be constant everywhere and equal to that of free space μ_0.

The current flowing in the larger transmitting loop is taken to be time-harmonic and equal to $Ie^{j\omega t}$, with ω being the angular frequency. Because of the symmetry of the problem, currents in the material medium flow only horizontally. This implies that the generated electric field has no vertical component, and as a consequence, the EM field is transverse electric (TE) with respect to the vertical direction (termed as $z-$ direction in the following) [5]. In this situation, it is well known that the magnetic field generated at the center of the two loops has only a vertical component, whose integral representation reads as [5].

$$H_z = \frac{Ib}{2}\int_0^\infty \left(1 + \frac{u_0 - u_1}{u_0 + u_1}e^{-2u_0 d}\right)\frac{\lambda^2}{u_0}J_1(\lambda b)d\lambda\,, \tag{1}$$

where b denotes the radius of the emitter and $J_m(\xi)$ is the m th-order Bessel function, and

$$u_n = \sqrt{\lambda^2 - k_n^2}, \tag{2}$$

$$k_n^2 = \omega^2\mu_n\epsilon_n - j\omega\mu_n\sigma_n. \tag{3}$$

And with the time-harmonic factor $e^{j\omega t}$ suppressed for notational simplicity. The aim of this paper is to derive exact series representations for H_z. To this goal, it is first convenient to use the differentiation properties of the Bessel functions and the identity

$$\frac{u_0 - u_1}{u_0 + u_1} = -1 + \frac{2u_0}{u_0 + u_1}, \tag{4}$$

so as to decompose (1) into three terms as follows:

$$H_z = -\frac{Ib}{2}\frac{\partial}{\partial b}\int_0^\infty \left(1 - e^{-2u_0 d} + \frac{2u_0}{u_0 + u_1}e^{-2u_0 d}\right)\frac{1}{u_0}J_0(\lambda b)\lambda\; d\lambda\,. \tag{5}$$

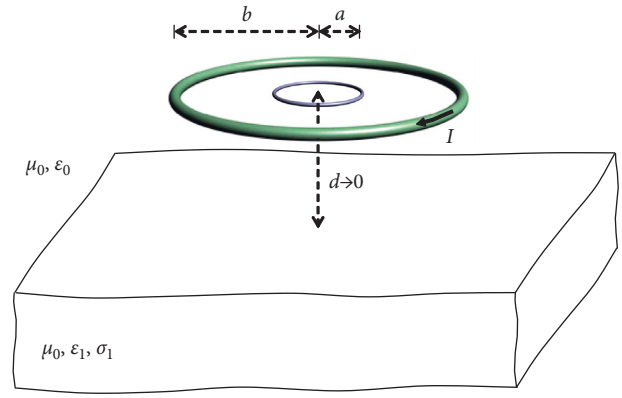

Figure 1: Two horizontal co-axial loops above a homogeneous ground.

The first two integrals on the right-hand side of (5) are special cases of the well-known tabulated Sommerfeld integral [19–23]

$$S_n(z) = \int_0^\infty \frac{e^{-u_n z}}{u_n}J_0(\lambda b)\lambda\; d\lambda = -jk_n h_0^{(2)}\left(k_n\sqrt{b^2 + z^2}\right), \tag{6}$$

and as a consequence, it yields the following:

$$H_z = \frac{jIk_0 b}{2}\frac{\partial}{\partial b}\left[h_0^{(2)}(k_0 b) - h_0^{(2)}(k_0 r) + \frac{2j}{k_0}\int_0^\infty \frac{e^{-2u_0 d}}{u_0 + u_1}J_0(\lambda b)\lambda \mathrm{d}\lambda\right], \tag{7}$$

with $r = \sqrt{b^2 + 4d^2}$. Next, to evaluate the last integral within the square brackets of (7), the numerator and denominator of the fraction in the integrand are first multiplied by $u_0 - u_1$. This leads to express (7) in the following form:

$$H_z = \frac{jIk_0 b}{2}\frac{\partial}{\partial b}\left[h_0^{(2)}(k_0 b) - h_0^{(2)}(k_0 r) + \frac{2j}{k_0}\frac{1}{k_1^2 - k_0^2}(P_0 - P_1)\right], \tag{8}$$

with

$$P_n = \int_0^\infty u_n e^{-2u_0 d}J_0(\lambda b)\lambda \mathrm{d}\lambda. \tag{9}$$

The explicit expression of P_0 may be found straightforwardly, since it is easily recognized to be related to $S_0(2h)$ in (6) by the following differential relation:

$$\begin{aligned} P_0 &= -\left[\frac{1}{b}\frac{\partial}{\partial b}\left(b\frac{\partial}{\partial b}\right) + k_0^2\right]S_0(2h) \\ &= jk_0\left[\frac{1}{b}\frac{\partial}{\partial b}\left(b\frac{\partial}{\partial b}\right) + k_0^2\right]h_0^{(2)}(k_0 r) \\ &= jk_0\left[k_0^2 h_0^{(2)}(k_0 r) - \frac{2k_0}{r}h_1^{(2)}(k_0 r) + \frac{k_0^2 b^2}{r^2}h_2^{(2)}(k_0 r)\right]. \end{aligned} \tag{10}$$

On the other hand, to evaluate P_1, it is convenient to rewrite it as follows:

$$P_1 = -\lim_{\delta \longrightarrow 0} \frac{\partial}{\partial \delta} \int_0^\infty e^{-u_1 \delta} e^{-2u_0 d} J_0(\lambda b) \lambda \mathrm{d}\lambda, \tag{11}$$

and then, change the variable of integration from λ to $\xi = (\lambda/|k_1|)$ and express u_0 as follows:

$$\begin{aligned} u_0 &= \sqrt{u_1^2 + k_1^2 - k_0^2} \\ &= |k_1| \sqrt{v_1^2 + \alpha}, \end{aligned} \tag{12}$$

where $v_1 = (u_1/|k_1|) = \sqrt{\xi^2 - \hat{k}_1^2}$ and $\alpha = \hat{k}_1^2 - \hat{k}_0^2$, being $\hat{k}_n = (k_n/|k_1|)$. This makes it possible to rewrite P_1 as follows:

$$P_1 = -|k_1|^2 \lim_{\delta \longrightarrow 0} \frac{\partial Q}{\partial \delta}, \tag{13}$$

where

$$Q = \int_0^\infty e^{-v_1 \hat{\delta}} e^{-2\hat{d}\sqrt{v_1^2 + \alpha}} J_0(\xi \hat{b}) \xi \mathrm{d}\xi, \tag{14}$$

and being $\hat{b} = |k_1| b$, $\hat{d} = |k_1| d$, and $\hat{\delta} = |k_1| \delta$. Next, since $|\alpha| < 1$, the exponential term of the integral may be replaced with its power series expansion with respect to α in Lommel's sense, namely,

$$e^{-\left(v_1 \hat{\delta} + 2\hat{d}\sqrt{v_1^2 + \alpha}\right)} = e^{-v_1 (2\hat{d} + \hat{\delta})} \left[\begin{array}{l} 1 - \dfrac{\hat{d}}{v_1} \alpha + \dfrac{\hat{d}\left(1 + 2v_1 \hat{d}\right)}{4v_1^3} \alpha^2 - \dfrac{\hat{d}\left(3 + 6v_1 \hat{d} + 4v_1^2 \hat{d}^2\right)}{24 v_1^5} \alpha^3 \\ \quad + \dfrac{\hat{d}\left(15 + 30 v_1 \hat{d} + 24 v_1^2 \hat{d}^2 + 8 v_1^3 \hat{d}^3\right)}{192 v_1^7} \alpha^4 + \cdots \end{array} \right], \tag{15}$$

where in the limit as $\delta \longrightarrow 0$, the quantity $2\hat{d}$ within the square brackets may be confused with $\hat{q} = 2\hat{d} + \hat{\delta}$. This makes it possible to turn (15) into the following:

$$\begin{aligned} e^{-\left(v_1 \hat{\delta} + 2\hat{d}\sqrt{v_1^2 + \alpha}\right)} &= e^{-v_1 \hat{q}} \left\{ 1 - \sum_{n=0}^{\infty} \frac{(-1)^n}{[2(n+1)]!!} \left(\frac{\alpha \hat{q}}{v_1} \right)^{n+1} \sum_{m=0}^{n} \frac{(v_1 \hat{q})^{-m}}{(2m)!!} \frac{(n+m)!}{(n-m)!} \right\} \\ &= e^{-v_1 \hat{q}} + j v_1 \hat{q} \sum_{n=0}^{\infty} \frac{1}{[2(n+1)]!!} \left(\frac{\alpha \hat{q}}{j v_1} \right)^{n+1} h_n^{(1)}(j v_1 \hat{q}), \end{aligned} \tag{16}$$

where $h_n^{(1)}$ is the n th-order spherical Hankel function of the first kind, which is defined as follows:

$$h_n^{(1)}(j v_1 \hat{q}) = -(-j)^n \frac{e^{-v_1 \hat{q}}}{v_1 \hat{q}} \sum_{m=0}^{n} \frac{(v_1 \hat{q})^{-m}}{(2m)!!} \frac{(n+m)!}{(n-m)!}. \tag{17}$$

Substitution of (16) into (14) provides the expression

$$\begin{aligned} Q = &-\left(\frac{\alpha \hat{q}}{2} + \frac{\partial}{\partial \hat{q}} \right) \int_0^\infty \frac{e^{-\hat{q} v_1}}{v_1} J_0(\xi \hat{b}) \xi \mathrm{d}\xi + \\ &j \hat{q} \sum_{n=1}^{\infty} \frac{1}{[2(n+1)]!!} (-j \alpha \hat{q})^{n+1} \int_0^\infty \frac{h_n^{(1)}(j \hat{q} v_1)}{v_1^n} J_0(\xi \hat{b}) \xi \mathrm{d}\xi, \end{aligned} \tag{18}$$

whose integrals on the right-hand side are known in the explicit form and tabulated in [19]. In particular, upon setting $\hat{R} = \sqrt{\hat{b}^2 + \hat{q}^2}$, we make use of the well-known result ([19] No. 13.47.2)

$$\int_0^\infty \frac{K_m(\hat{q} v_1)}{v_1^m} J_0(\xi \hat{b}) \xi \mathrm{d}\xi = \frac{1}{\hat{q}} \left(\frac{\hat{R}}{j \hat{k}_1 \hat{q}} \right)^{m-1} K_{m-1}\left(j \hat{k}_1 \hat{R} \right), \tag{19}$$

with $K_m(\cdot)$ being the m th-order modified Bessel function of the second kind and $m = n + (1/2)$, in combination with the identities [24]

$$\begin{aligned} K_{n+(1/2)}(\hat{q} v_1) &= \frac{\pi}{2} j^{n+(3/2)} H_{n+(1/2)}^{(1)}(j \hat{q} v_1) \\ &= -j^n \sqrt{\frac{\pi \hat{q} v_1}{2}} h_n^{(1)}(j \hat{q} v_1) - \pi < \arg(\hat{q} v_1) \le \frac{\pi}{2}, \end{aligned} \tag{20}$$

$$\begin{aligned} K_{n-(1/2)}\left(j \hat{k}_1 \hat{R} \right) &= \frac{\pi}{2} (-j)^{n+(1/2)} H_{n-(1/2)}^{(2)}\left(\hat{k}_1 \hat{R} \right) \\ &= (-j)^{n+(1/2)} \sqrt{\frac{\pi \hat{k}_1 \hat{R}}{2}} h_{n-1}^{(2)}\left(\hat{k}_1 \hat{R} \right) \\ &\quad -\frac{\pi}{2} < \arg\left(j \hat{k}_1 \hat{R} \right) \le \pi, \end{aligned} \tag{21}$$

allows to obtain the expression

$$\int_0^{\infty} \frac{h_n^{(1)}(j\widehat{q}v_1)}{v_1^n} J_0(\xi\widehat{b})\xi \mathrm{d}\xi = \frac{1}{\widehat{q}}\left(-\frac{\widehat{R}}{j\widehat{k}_1\widehat{q}}\right)^{n-(1/2)} \sqrt{\frac{j\widehat{k}_1\widehat{R}}{\widehat{q}}} h_{n-1}^{(2)}\left(\widehat{k}_1\widehat{R}\right), \tag{22}$$

that is, equivalently,

$$\int_0^{\infty} \frac{h_n^{(1)}(j\widehat{q}v_1)}{v_1^n} J_0(\xi\widehat{b})\xi \mathrm{d}\xi = \frac{\widehat{k}_1}{\widehat{q}}\left(-\frac{\widehat{R}}{j\widehat{k}_1\widehat{q}}\right)^{n} h_{n-1}^{(2)}\left(\widehat{k}_1\widehat{R}\right), \tag{23}$$

which leads to express (18) as follows:

$$Q = Q_0 + \sum_{n=1}^{\infty} \frac{1}{[2(n+1)]!!} \frac{\alpha^{n+1}}{\widehat{k}_1^{n-1}} \widehat{q}\widehat{R}^n h_{n-1}^{(2)}\left(\widehat{k}_1\widehat{R}\right). \tag{24}$$

with

$$\begin{aligned} Q_0 &= -\left(\frac{\alpha\widehat{q}}{2} + \frac{\partial}{\partial\widehat{q}}\right)\frac{e^{-j\widehat{k}_1\widehat{R}}}{\widehat{R}} \\ &= j\widehat{k}_1\widehat{q}\left[\frac{\alpha}{2}h_0^{(2)}\left(\widehat{k}_1\widehat{R}\right) - \frac{\widehat{k}_1}{\widehat{R}}h_1^{(2)}\left(\widehat{k}_1\widehat{R}\right)\right]. \end{aligned} \tag{25}$$

Making use of (24) into (13) provides the following:

$$P_1 = -|k_1|^2 \lim_{\delta\longrightarrow 0}\left\{\frac{\partial Q_0}{\partial\delta} + \sum_{n=1}^{\infty}\frac{1}{[2(n+1)]!!}\frac{\alpha^{n+1}}{\widehat{k}_1^{n-1}}\frac{\partial}{\partial\delta}\left[\widehat{q}\widehat{R}^n h_{n-1}^{(2)}\left(\widehat{k}_1\widehat{R}\right)\right]\right\}, \tag{26}$$

and, upon introducing the differentiation properties of the spherical Bessel functions, namely ([24], No. 10.1.23, 10.1.24),

$$\frac{\mathrm{d}}{\mathrm{d}\widehat{R}}\left[\widehat{R}^{-n}h_n^{(2)}\left(\widehat{k}_1\widehat{R}\right)\right] = -\widehat{k}_1\frac{h_{n+1}^{(2)}\left(\widehat{k}_1\widehat{R}\right)}{\widehat{R}^n}, \tag{27}$$

$$\frac{\mathrm{d}}{\mathrm{d}\widehat{R}}\left[\widehat{R}^n h_{n-1}^{(2)}\left(\widehat{k}_1\widehat{R}\right)\right] = \widehat{k}_1\widehat{R}^n h_{n-2}^{(2)}\left(\widehat{k}_1\widehat{R}\right), \tag{28}$$

it is straightforward to conclude that

$$\frac{\partial Q_0}{\partial\widehat{\delta}} = j\widehat{k}_1\left\{\frac{\alpha}{2}h_0^{(2)} + \frac{\widehat{k}_1}{\widehat{R}}\left[-\left(1+\frac{\alpha\widehat{q}^2}{2}\right)h_1^{(2)} + \widehat{k}_1\widehat{q}h_2^{(2)}\right]\right\}, \tag{29}$$

$$\frac{\partial}{\partial\widehat{\delta}}\left[\widehat{q}\widehat{R}^n h_{n-1}^{(2)}\right] = \widehat{R}^n\left[h_{n-1}^{(2)} + \frac{\widehat{k}_1\widehat{q}^2}{\widehat{R}}h_{n-2}^{(2)}\right], \tag{30}$$

where the argument $\widehat{k}_1\widehat{R}$ of the spherical Hankel functions has been omitted for notational simplicity. Thus, after taking the limit as $\delta \longrightarrow 0$, it turns out that $\widetilde{R} = |k_1|r$, $\widetilde{k}_1\widetilde{R} = k_1 r$, and

$$P_1 = k_1^3\left(P_1' + P_1''\right), \tag{31}$$

where

$$P_1' = \frac{1-\tau^2}{2j}h_0^{(2)}(k_1r) - \frac{1}{jk_1r}\left\{\left[1+2\left(k_1^2-k_0^2\right)d^2\right]h_1^{(2)}(k_1r) - 2k_1dh_2^{(2)}(k_1r)\right\}, \tag{32}$$

$$P_1'' = -\sum_{n=1}^{\infty}\frac{\left(1-\tau^2\right)^{n+1}}{[2(n+1)]!!}(k_1r)^n\left[h_{n-1}^{(2)}(k_1r) + \frac{4k_1d^2}{r}h_{n-2}^{(2)}(k_1r)\right], \tag{33}$$

and with $\tau = (k_0/k_1)$. Use of (10) in conjunction with (31)–(33) into (8) provides, after performing the b–derivatives of the spherical Hankel functions, the following expression for the H_z–field calculated at the center of the loops

$$H_z = \frac{jIk_0^2b^2}{2r}\left[-\frac{r}{b}h_1^{(2)}(k_0b) + h_1^{(2)}(k_0r) + \widetilde{P}_0 + \frac{1}{k_0r\tau}\widetilde{P}_1\right], \tag{34}$$

being

$$\widetilde{P}_0 = \frac{2\tau^2}{1-\tau^2}\left[h_1^{(2)}(k_0r) - \frac{4}{k_0r}h_2^{(2)}(k_0r) + \frac{b^2}{r^2}h_3^{(2)}(k_0r)\right], \tag{35}$$

$$\begin{aligned} \widetilde{P}_1 = {} & k_1rh_1^{(2)}(k_1r) - \frac{2}{1-\tau^2}\left\{\left[1+2\left(k_1^2-k_0^2\right)d^2 + \frac{2\,d}{r}\right]h_2^{(2)}(k_1r) - 2k_1dh_3^{(2)}(k_1r)\right\} \\ & + 2j\sum_{n=1}^{\infty}\frac{\left(1-\tau^2\right)^n}{[2(n+1)]!!}(k_1r)^{n+1}\left[h_{n-2}^{(2)}(k_1r) + \frac{4k_1d^2}{r}h_{n-3}^{(2)}(k_1r)\right]. \end{aligned} \tag{36}$$

Finally, since the radius a of the receiver has been assumed to be sufficiently small, this implies that $k_0a \ll 1$ and $a \ll b$; it turns out that the voltage induced in the receiver is given by (34) multiplied by $j\omega\mu_0\pi a^2$.

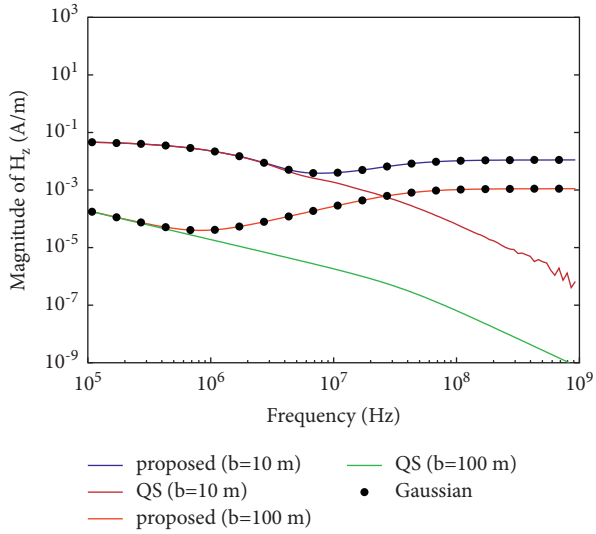

FIGURE 2: Amplitude-frequency spectrum of the H_z–field at the center of the two loops.

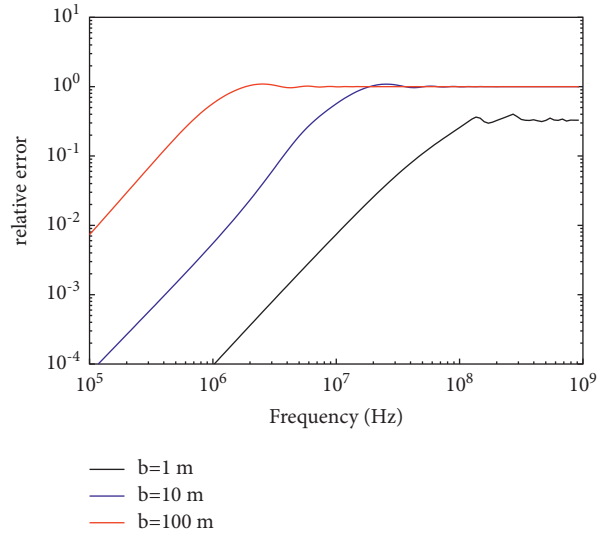

FIGURE 3: Relative error of the outcomes of (37) as compared to the results from (34), plotted against frequency.

3. Numerical Results

In this section, the results arising from (34) are compared with those provided by the previously published quasistatic solution to the considered problem, namely [5],

$$H_z = -\frac{I}{k_1^2 b^3}\left[3 - \left(3 + 3jk_1 b - k_1^2 b^2\right)e^{-jk_1 b}\right], \qquad (37)$$

which is obtained by assuming that both the emitter and the receiver lie on the top surface of the conducting medium to be explored (that is by assuming $d = 0$). For the sake of validation of the proposed formulation, the results generated by (34) are also compared with the data arising from numerical integration of (1), performed by using an adaptive Gauss–Kronrod G7-K15 quadrature rule, resulting from the combination of a 7-point Gauss rule with a 15-point Kronrod rule. In particular, after mapping the semi-infinite integration interval onto the finite interval $[0:1]$ through a suitable change of variable, the latter interval has been recursively decomposed until the estimates of the relative errors associated with all the sub-integrals, each one given by the relative difference between the Gaussian and Kronrod rule [25], do not exceed a fixed tolerance level.

First, the three different approaches are applied to the computation of the amplitude-frequency spectrum of the H_z–field produced at the center of a loop carrying 1 A of current and placed on a clay soil. The index N at which the infinite sum in (36) is terminated is taken to be equal to 15, while two distinct values for the radius b of the source loop are considered, that is, $b = 10$ m and $b = 100$ m. Finally, the electrical conductivity and dielectric permittivity of the clay soil are taken to be $\sigma_1 = 10$ mS/m and $\epsilon_1 = 10\,\epsilon_0$ [8], respectively. The obtained curves, illustrated in Figure 2, show how the numerical data agree well with the outcomes of (34) all over the considered frequency interval. Thus, the results from (34) may be referred to as exact curves. Conversely, discrepancy is observed between the quasistatic and exact

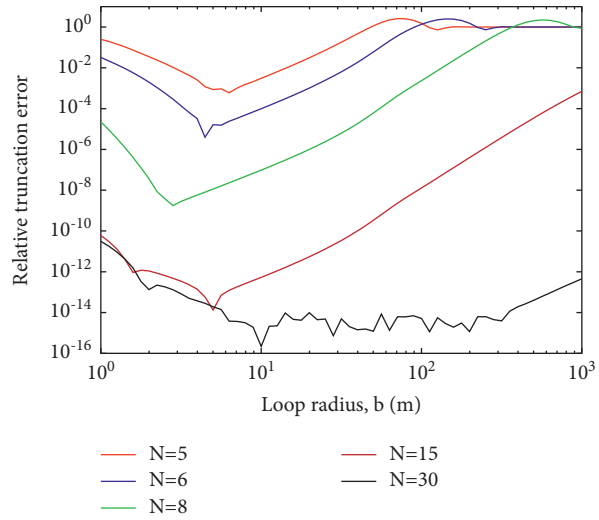

FIGURE 4: Relative truncation error of (34) against the radius of the source loop, with the truncation index N taken as a parameter.

trends even in the low-frequency range, to a greater extent the larger the radius of the source loop. Moreover, the quasistatic curves start to deviate from the exact ones at the frequencies of about 3 MHz when $b = 10$ m, and 300 kHz for $b = 100$ m. This means that the extension of the quasistatic frequency range decreases as b is increased.

The decrease in accuracy of the quasistatic solution as frequency grows up is further illustrated in Figure 3, which shows the relative error originating from substituting (37) in place of (34)–(36) with $N = 15$, which is again plotted against frequency. Here, the electromagnetic parameters of the material medium are given the same values as in the previous example. From the analysis of the plotted curves, it is found that the relative error increases almost linearly in the low-frequency range, up to the limits of about 100% for

Table 1: CPU time comparisons for the computation of the H_z–field.

Loop radius (m)	Approach	Relative error	CPU time (s)
100	G7-K15 (Tol = 10^{-7})	$0.48 \cdot 10^{-7}$	8.3
100	Proposed solution ($N = 15$)	$0.13 \cdot 10^{-7}$	0.336
500	G7-K15 (Tol = 10^{-12})	$0.67 \cdot 10^{-13}$	17.4
500	Proposed solution ($N = 15$)	$0.35 \cdot 10^{-4}$	0.372
500	Proposed solution ($N = 30$)	$0.4 \cdot 10^{-13}$	1.19

$b = 10$ m and $b = 100$ m, and 30% for $b = 1$ m. This implies that the quasistatic solution exhibits a higher accuracy if the radius of the source coil is reduced. Once the upper limit is reached, the error generated by (37) does not change any longer with increasing frequency.

One would ask how quickly (34) converges to the exact solution for different values of the radius b of the source loop. This aspect is investigated by Figure 4, which depicts the relative truncation error that results from using (34) with a truncated sum in place of the infinite sum, plotted against b with the truncation index N taken as a parameter. The operating frequency is assumed to be equal to 100 kHz, and the estimate of the infinite sum is obtained by terminating the sequence of partial sums when the relative difference between the two last partial sums is smaller than 10^{-14}. The same material medium as in the preceding examples is considered. A glance at Figure 4 reveals that convergence is in general slower for small but especially for large values of b. For instance, if $b = 100$ m it suffices to use a sum made up of $N = 15$ terms to get an acceptable relative truncation error ($1.3 \cdot 10^{-8}$), but as b is further increased the accuracy of the result of the computation rapidly drops, and it can be enhanced only by increasing the truncation order (up to $N = 30$, as an example). However, the need to resort to longer sums does not imply that the proposed approach is more computationally expensive than numerical integration. In fact, with accuracy being equal, the time cost of the analytical approach is always smaller than that of numerical integration. The validity of this statement is confirmed by the entries of Table 1, which shows the time taken by (34) and the Gauss–Kronrod scheme, on a standard 1.8 GHz processor, to determine the H_z–field produced for $b = 100$ m and $b = 500$ m. The estimate of the relative error generated by Gauss-Kronrod rule and the relative truncation error associated with (34) are also indicated in the third column of Table 1. As can be observed, for $b = 100$ m, the use of (34) with $N = 15$ ensures approximately the same level of accuracy offered by numerical quadrature, but with significant timesaving with respect to the latter. On the other hand, when $b = 500$ m, the relative error associated with $N = 15$ is no longer small, and longer sums must be used in order to improve accuracy.

The entries of Table 1 confirm that increasing N up to 30 permits breaking down the truncation error and, at the same time, tell us that the improvement in accuracy is not achieved at the cost of significantly worsening the computation time, which is still far smaller than that implied by a numerical scheme which offers the same degree of precision.

It has been shown how increasing the radius b of the source loop reduces the frequency range of validity of the quasistatic assumption, and that at higher frequencies, the quasistatic solution fails regardless of the value of b. The only exception to this rule occurs when the loops lie on a poorly conducting ground. This point is clarified by Figure 5, which illustrates profiles of the voltage induced in the small receiving loop against the conductivity σ_1, calculated by assuming $\epsilon_1 = 10\,\epsilon_0$ and $a = 5$ cm. The operating frequency is taken to be 100 MHz, and the same values for b as in the previous example are considered.

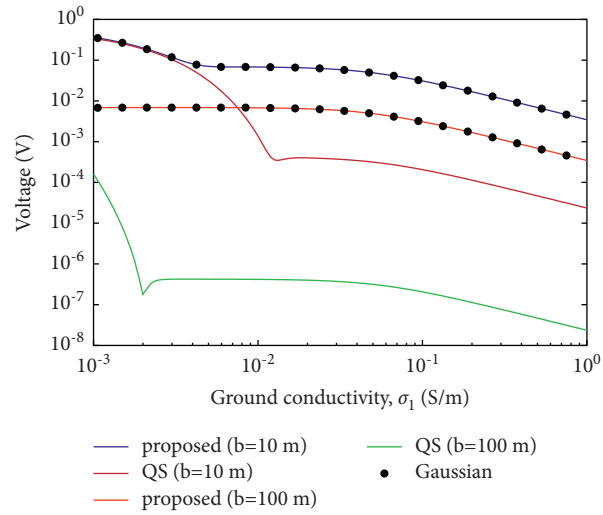

Figure 5: Voltage induced in the small loop as a function of the ground conductivity.

As is seen, for larger source loops ($b = 100$ m), there is no chance to obtain accurate results by using the quasistatic solution for the voltage, and this is expected because of the relatively high operating frequency. Conversely, for $b = 10$ m, the quasistatic assumption still holds at 100 MHz, provided that the ground conductivity σ_1 does not exceed few mS/m.

4. Conclusion

The purpose of the present work has been to derive the exact explicit expression describing the time-harmonic voltage response of a central loop electromagnetic sounding system placed on a homogeneous earth structure. The solution has been obtained by turning the semi-infinite integral representation for the vertical magnetic field induced at the center of the emitter into a series of simpler integrals amenable to analytical evaluation. The series expansion of the field integral has been made possible by the replacement of the exponential term of the integrand with its power series

expansion with respect to the difference of the squares of the wavenumbers in air and in the conducting medium. As a result, the vertical magnetic field and the induced voltage have been expressed in terms of the spherical Hankel functions of the wavenumbers and geometrical parameters. The results of numerical tests have shown the validity of the proposed approach. In particular, it has been seen how the derived solution exhibits advantages in terms of time cost and accuracy, when compared, respectively, to the numerical quadrature rules devoted to the evaluation of the Sommerfeld-type integrals, and to the previously published quasistatic solution to the problem.

Data Availability

No data are available.

Conflicts of Interest

The authors declare that they have no conflicts of interest.

References

[1] F. Kong, S. Johnstad, and J. Park, "Wavenumber of the guided wave supported by a thin resistive layer in marine controlled-source electromagnetics," *Geophysical Prospecting*, vol. 58, no. 4, pp. 711–723, 2010.

[2] V. Tamburrelli and M. Salis, "Efficient evaluation of the time-harmonic response in central loop electromagnetic sounding," *Progress In Electromagnetics Research Letters*, vol. 96, pp. 53–58, 2021.

[3] W. Menke, *Geophysical Data Analysis: Discrete Inverse Theory*, Academic Press, Cambridge, MA, USA, 2018.

[4] J. R. Wait, "Mutual electromagnetic coupling of loops over a homogeneous ground," *Geophysics*, vol. 20, no. 3, pp. 630–637, 1955.

[5] S. H. Ward and G. W. Hohmann, "Electromagnetic theory for geophysical applications," *Electromagnetic Methods in Applied Geophysics*, vol. 1, pp. 130–311, 1988.

[6] B. R. Spies and F. C. Frischknecht, "Electromagnetic sounding," *Electromagnetic Methods in Applied Geophysics*, vol. 2, pp. 285–426, 1988.

[7] W. M. Telford, L. P. Geldart, and R. E. Sheriff, "Applied geophysics," *Cambridge University Press*, vol. 1, 1990.

[8] G. J. Palacky, "Resistivity characteristics of geologic targets," *Electromagnetic Methods in Applied Geophysics*, vol. 1, pp. 52–129, 1988.

[9] M. Parise, "On the surface fields of a small circular loop antenna placed on plane stratified earth," *International Journal of Antennas and Propagation*, vol. 2015, Article ID 187806, 8 pages, 2015.

[10] N. P. Singh and T. Mogi, "Electromagnetic response of a large circular loop source on a layered earth: a new computation method," *Pure and Applied Geophysics*, vol. 162, no. 1, pp. 181–200, 2005.

[11] J. R. Wait, "Fields of a horizontal loop antenna over a layered half-space," *Journal of Electromagnetic Waves and Applications*, vol. 9, no. 10, pp. 1301–1311, 1995.

[12] M. Parise, M. Muzi, and G. Antonini, "Loop antennas with uniform current in close proximity to the earth: canonical solution to the surface-to-surface propagation problem," *Progress in Electromagnetics Research B*, vol. 77, pp. 57–69, 2017.

[13] N. P. Singh and T. Mogi, "Effective skin depth of em fields due to large circular loop and electric dipole sources," *Earth Planets and Space*, vol. 55, no. 6, pp. 301–313, 2003.

[14] M. Parise, "Full-wave analytical explicit expressions for the surface fields of an electrically large horizontal circular loop antenna placed on a layered ground," *IET Microwaves, Antennas & Propagation*, vol. 11, no. 6, pp. 929–934, 2017.

[15] N. Singh and T. Mogi, "EMLCLLER-a program for computing the em response of a large loop source over a layered earth model," *Computers & Geosciences*, vol. 29, no. 10, pp. 1301–1307, 2003.

[16] M. Parise, V. Tamburrelli, and G. Antonini, "Mutual impedance of thin-wire circular loops in near-surface applications," *IEEE Transactions on Electromagnetic Compatibility*, vol. 61, no. 2, pp. 558–563, 2019.

[17] N. L. Shastri and H. P. Patra, "Multifrequency sounding results of laboratory simulated homogeneous and two-layer earth models," *IEEE Transactions on Geoscience and Remote Sensing*, vol. 26, no. 6, pp. 749–752, 1988.

[18] M. Parise, "Efficient computation of the surface fields of a horizontal magnetic dipole located at the air-ground interface," *International Journal of Numerical Modelling: Electronic Networks, Devices and Fields*, vol. 29, no. 4, pp. 653–664, 2016.

[19] G. N. Watson, *A Treatise on the Theory of Bessel Functions, Ser. Cambridge Mathematical Library*, Cambridge University Press, Cambridge, UK, 1944.

[20] M. Parise, "Exact EM field excited by a short horizontal wire antenna lying on a conducting soil," *AEU-International Journal of Electronics and Communications*, vol. 70, no. 5, pp. 676–680, 2016.

[21] M. Parise, "Transverse magnetic field of infinite line source placed on ground surface," *Electronics Letters*, vol. 51, no. 19, pp. 1478–1480, 2015.

[22] M. Parise, "Improved Babylonian square root algorithm-based analytical expressions for the surface-to-surface solution to the Sommerfeld half-space problem," *IEEE Transactions on Antennas and Propagation*, vol. 63, no. 12, pp. 5832–5837, 2015.

[23] M. Parise and G. Antonini, "On the radiation from a short current-carrying straight wire oriented perpendicular to a stratified medium," *Progress in Electromagnetics Research*, vol. 159, pp. 49–57, 2017.

[24] M. Abramowitz and I. A. Stegun, "Handbook of mathematical functions: with formulas, graphs, and mathematical tables," *Journal of the American Statistical Association*, vol. 59, no. 308, 1324 pages, 1964.

[25] S. Venkateshan and P. Swaminathan, *Computational Methods in Engineering*, Elsevier, Amsterdam, Netherlands, 2013.